Eur. Phys. J. C (2017) 77:390
DOI 10.1140/epjc/s10052-017-4966-7

THE EUROPEAN PHYSICAL JOURNAL C

Regular Article - Theoretical Physics

Thermodynamical and dynamical properties of charged BTZ black holes

Zi-Yu Tang[1,a], **Cheng-Yong Zhang**[2,b], **Mahdi Kord Zangeneh**[1,3,4,5,c], **Bin Wang**[1,d], **Joel Saavedra**[6,e]

[1] Department of Physics and Astronomy, Center for Astronomy and Astrophysics, Shanghai Jiao Tong University, Shanghai 200240, China
[2] Center for High-Energy Physics, Peking University, Beijing 100871, China
[3] Physics Department, Faculty of Science, Shahid Chamran University of Ahvaz, Ahvaz 61357-43135, Iran
[4] Research Institute for Astronomy and Astrophysics of Maragha (RIAAM)-Maragha, P. O. Box: 55134-441, Maragha, Iran
[5] Physics Department and Biruni Observatory, College of Sciences, Shiraz University, Shiraz 71454, Iran
[6] Instituto de Fisica, Pontificia Universidad Catolica de Valparaiso, Casilla 4950, Valparaiso, Chile

Received: 20 April 2017 / Accepted: 30 May 2017 / Published online: 13 June 2017

Abstract We investigate the spacetime properties of BTZ black holes in the presence of the Maxwell field and Born–Infeld field and find rich properties in the spacetime structures when the model parameters are varied. Employing Landau–Lifshitz theory, we examine the thermodynamical phase transition in the charged BTZ black holes. We further study the dynamical perturbation in the background of the charged BTZ black holes and find different properties in the dynamics when the thermodynamical phase transition occurs.

1 Introduction

The discovery of three-dimensional black holes by Bañados, Teitelboim and Zanelli (BTZ black holes) [1] has been known as one of the greatest achievements in the study of gravity. The BTZ black hole provides us a framework to understand gravitational interactions in low-dimensional spacetimes [2]. It also accommodates a simpler setting to explore many of the mysteries of black hole statistical mechanics in higher dimensions [3]. In three spacetime dimensions, general relativity becomes a topological field theory, whose dynamics can be largely described holographically by a two-dimensional conformal field theory at the boundary of spacetime [3]. Thus the BTZ black hole is a natural environment to realize the idea of AdS/CFT correspondence. It was found that quasi-normal modes determining the relaxation time of rotating BTZ black hole perturbations are exactly in agreement with the location of the poles of the retarded correlation function of the corresponding perturbations in the dual conformal field theory [4]. This serves as a quantitative test of the AdS/CFT correspondence; for a review see [5,6] and the references therein on this topic.

Considerable progress has been made for the study of BTZ black holes where gravity minimally coupled to matter fields [3,7]. When the 2+1 gravity is coupled to electromagnetism, we have the charged BTZ black hole solution [1]. But compared with the neutral holes, the charged BTZ black hole has not been thoroughly investigated. One of the possible reasons is that the charged BTZ black hole is not a spacetime of constant curvature [8]. This makes the analysis in terms of identifications in AdS space not applicable for charged BTZ black holes [8], which becomes an obstacle to understand the geometrical properties there. Another reason is that there is a logarithmic function in the metric expression of the charged BTZ black hole, which makes the analytic investigation difficult.

The motivation of this work is to study carefully the charged BTZ black holes and present clearly the physical properties once enveiled by mathematical difficulty. We will first concentrate on the charged BTZ black hole solutions obtained from the standard Einstein–Maxwell equations in 2+1 spacetime dimensions with a negative cosmological constant. Then we will generalize our discussions to charged BTZ black holes obtained when the nonlinear Born–Infeld (BI) electromagnetism is brought in [9,10]. The Born–Infeld theory (BI theory) was first introduced to solve infinite self-energy problem by imposing a maximum strength of the electromagnetic field [11]. The generalization of the Maxwell field to nonlinear electrodynamics will lead to new solutions and introduce new phenomena to the system under consideration [11]. It is of great interest to investigate how the highly

[a] e-mail: tangziyu@sjtu.edu.cn
[b] e-mail: zhangcy0710@pku.edu.cn
[c] e-mail: mkzangeneh@shirazu.ac.ir
[d] e-mail: wang_b@sjtu.edu.cn
[e] e-mail: joel.saavedra@pucv.cl

nonlinear corrections to the gauge matter fields influence the bulk black hole spacetime structure and its dynamical and thermodynamical properties in $2+1$ gravity.

In this paper we will first go over charged BTZ black hole solutions with standard Maxwell field and nonlinear BI field. We will discuss the spacetime structures, and disclose rich spacetime properties of the black hole in the presence of the charge parameter. The strength of the charge parameter determines whether the phase transition can happen or not. We will further use the Landau–Lifshitz theory for thermodynamic fluctuations to discuss the thermodynamical phase transitions in the charged BTZ black holes. We will show that some second moments diverge in the extreme limit, indicating that thermodynamical phase transition occurs.

It was argued that at the phase transition point, when the nonextreme black hole becomes extreme, the Hawking temperature is zero which indicates that for the extreme black hole there is only superradiation but no Hawking radiation, which is greatly different from that of the nonextreme black holes. Different radiation properties between extreme and nonextreme black holes were used as an indication of the occurrence of the second-order phase transition [12–14].

However, there are some other discussions on Hawking radiation when the Hawking temperature is zero [15,16]. For a sufficiently low black hole temperature, Hiscock and Weems modeled the evaporation of a four-dimensional asymptotically flat charged black hole by $\frac{\mathrm{d}M}{\mathrm{d}t} = -\alpha a T^4 \sigma + \frac{Q}{r_h}\frac{\mathrm{d}Q}{\mathrm{d}t}$. They emphasized that charged particles emission can be modeled separately from the thermal Hawking flux of neutral particles, but they are all part of Hawking radiation. This is because emission of charged particle is thermodynamically related to a chemical potential associated with the electromagnetic field of the black hole. Even in the limit $T = 0$, the mass loss occurs from $\frac{\mathrm{d}Q}{\mathrm{d}t}$ term alone due to pair production by the Schwinger effect. The presence of particle production at zero temperature can also be read from Hawking's original formula $\langle N_{j\omega lp}\rangle = \frac{\Gamma_{j\omega lp}}{exp((\omega - e\Phi)/T) \pm 1}$ of [17] for the number of particle emission. See also Gibbons [18] for discussions regarding emission from a charged black hole.

These subtleties regarding particle emission when Hawking temperature is zero make the classification of different phases in nonextreme and extreme black holes through different radiation properties somewhat subtle and difficult. Then there comes a question whether there are some other phenomena to indicate the sharp difference when the phase transition occurs between the nonextreme and extreme black holes. This serves as another motivation of the present paper. We will focus on the dynamical properties of the charged BTZ black holes by studying the quasi-normal modes of scalar perturbation. We find that QNMs can serve as another probe for the phase transition between the nonextreme and extreme black holes. The results tell us that the extreme charged BTZ black hole is easily destroyed if we add more perturbations to the system, while the nonlinearity of the electromagnetic field can protect the black hole spacetime partially and make the perturbation outside the black hole decay faster.

2 Charged BTZ black hole solutions

In this section, we first review the derivation of charged BTZ black hole solutions in the presence of linear Maxwell (LM) [1] and nonlinear Born–Infeld (BI) [9] electrodynamics. Then we discuss the spacetime properties of these charged BTZ black holes.

Let us begin with the action of Einstein gravity in the presence of a gauge field,

$$S_{\mathrm{grav}} = S_{\mathrm{EH}} + S_{\mathrm{gauge}} + S_{\mathrm{GH}}, \tag{1}$$

where S_{EH}, S_{gauge} and S_{GH} are the Einstein–Hilbert, gauge field and Gibbons–Hawking actions defined as

$$S_{\mathrm{EH}} = -\frac{1}{16\pi}\int_M d^3x\sqrt{-g}\left(R + \frac{2}{l^2}\right), \tag{2}$$

$$S_{\mathrm{gauge}} = -\frac{1}{16\pi}\int_M d^3x\sqrt{-g}L(F), \tag{3}$$

$$S_{\mathrm{GH}} = -\frac{1}{8\pi}\int_{\partial M} d^2x\sqrt{-h}K, \tag{4}$$

in which R is the Ricci scalar for the bulk manifold M, l is the AdS radius and $L(F)$ is the Lagrangian of electrodynamic field $F_{\mu\nu}$ where $F = F_{\mu\nu}F^{\mu\nu}$, $F_{\mu\nu} = \partial_{[\mu}A_{\nu]}$ and A_ν is the electrodynamic gauge potential. h is the determinant of the two-dimensional metric on the boundary of manifold M (∂M) and K is the trace of the extrinsic curvature of the boundary. The Lagrangians of the electrodynamic field for linear Maxwell and nonlinear BI cases are

$$L(F) = \begin{cases} -F & \mathrm{LM} \\ 4\beta^2\left(1 - \sqrt{1 + \frac{F}{2\beta^2}}\right) & \mathrm{BI} \end{cases}, \tag{5}$$

where β is the parameter of nonlinearity. Nonlinear BI electrodynamics reduces to the linear Maxwell case when $\beta \to \infty$. Varying the action (1) with respect to the metric $g_{\mu\nu}$ and the gauge potential A_μ, we obtain

$$R_{\mu\nu} - \frac{1}{2}g_{\mu\nu}\left(R + \frac{2}{l^2}\right) = \frac{1}{2}g_{\mu\nu}L(F) - 2F_{\mu\sigma}F^{\sigma}_{\nu}\frac{\mathrm{d}L(F)}{\mathrm{d}F}, \tag{6}$$

$$\partial_\mu\left(\sqrt{-g}\frac{\mathrm{d}L(F)}{\mathrm{d}F}F^{\mu\nu}\right) = 0. \tag{7}$$

Substituting the gauge potential $A_\mu = \varphi(r)\delta^0_\mu$ into Eq. (7), we obtain the nonvanishing component of the electrodynamic field tensor,

$$F_{tr} = -F_{rt} = \frac{q}{r} \times \begin{cases} 1 & \text{LM}, \\ \Gamma^{-1} & \text{BI}, \end{cases} \tag{8}$$

where q is a constant related to the total charge of the black hole and $\Gamma = \sqrt{1 + q^2/\left(r^2\beta^2\right)}$. Equation (6) admits the charged BTZ black hole solution as

$$\mathrm{d}s^2 = -f(r)\mathrm{d}t^2 + \frac{\mathrm{d}r^2}{f(r)} + r^2\mathrm{d}\theta^2, \tag{9}$$

in which

$$f(r) = \frac{r^2}{l^2} - m + \begin{cases} -2q^2 \ln\frac{r}{l} & \text{LM}, \\ 2r^2\beta^2\left(1-\Gamma\right) + q^2\left[1 - 2\ln\left(r\frac{(1+\Gamma)}{2l}\right)\right] & \text{BI}, \end{cases} \tag{10}$$

where m is a constant which is proportional to the total mass of the black hole and can be obtained by using the fact that metric function vanishes at the event horizon r_+

$$m = \begin{cases} \frac{r_+^2}{l^2} - 2q^2\ln\left(\frac{r_+}{l}\right) & \text{LM}, \\ \frac{r_+^2}{l^2} + 2r_+^2\beta^2\left(1-\Gamma_+\right) + q^2\left[1 - 2\ln\left(r_+\frac{(1+\Gamma_+)}{2l}\right)\right] & \text{BI}, \end{cases} \tag{11}$$

where $\Gamma_+ = \sqrt{1 + q^2/\left(r_+^2\beta^2\right)}$.

In the following, we will explore the spacetime properties of linearly and nonlinearly charged BTZ black holes.

2.1 Linearly charged BTZ black holes

The metric function for the linearly charged BTZ black hole reads

$$f(r) = \frac{r^2}{l^2} - m - 2q^2\ln\frac{r}{l}. \tag{12}$$

In [10], it was argued that for fixed parameters $l = 1$ and $q = 1$, there is a naked singularity when m is sufficiently small, while the mass parameter is at a critical value, there is an extreme BTZ black hole. When the mass is above the critical value, the charged BTZ black hole can have two horizons enveloping the central singularity, namely the inner Cauchy horizon r_- and the outer event horizon r_+.

How about the situation if we treat q as a variable? The answer was not provided in [10]. In order to study the extreme charged BTZ black hole, we first let the metric function $f(r)$ to be zero which can tell us the location of the horizon. Furthermore we require the derivative of the metric function $f'(r)$ to vanish at the horizon which ensures the extremal condition to be satisfied. From these conditions,

$$\begin{aligned} f(r_{+\text{ext}}) &= \frac{r_{+\text{ext}}^2}{l^2} - m_{\text{ext}} - 2q_{\text{ext}}^2\ln\frac{r_{+\text{ext}}}{l} = 0, \text{ and} \\ f'(r_{+\text{ext}}) &= \frac{2r_{+\text{ext}}}{l^2} - \frac{2q_{\text{ext}}^2}{r_{+\text{ext}}} = 0, \end{aligned} \tag{13}$$

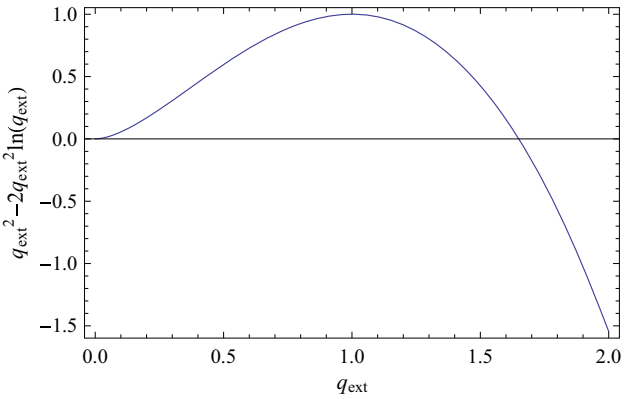

Fig. 1 The behavior of the left-hand side of Eq. (14) versus q. There is a maximum at $q_{\text{ext}} = 1$

we have an equation relating q_{ext} and m_{ext}

$$q_{\text{ext}}^2 - 2q_{\text{ext}}^2\ln q_{\text{ext}} = m_{\text{ext}}. \tag{14}$$

The behavior of the left-hand side of Eq. (14) is shown in Fig. 1, which has a peak equaling to one when $q = 1$. When $m = 1$, there is only one solution of Eq. (14), which is at $q = 1$ and the charged BTZ black hole is extreme. When $0 < m < 1$, there will be two solutions for q_{ext} from Eq. (14). The black hole can be extreme for these two charge values when $m < 1$. However, when $m > 1$, there is no solution of (14), which indicates that the extreme black hole condition cannot be respected so that the charged BTZ black hole is always nonextreme when $m > 1$.

To have a clearer picture, we plot the metric function $f(r)$ in Fig. 2 for different values of m. For $m < 1$ (we choose $m = 0.5$), we have two values q_1 and q_2 to accommodate the extreme black hole. We can see From Fig. 2a that when $q < q_1$ and $q > q_2$, the black hole is nonextreme with two horizons. But in the range $q_1 < q < q_2$, there is no root of the metric function so that the black hole does not exist. When $m = 1$, we see that there is just one value for the critical charge, namely $q = 1$, to accommodate the extreme charged BTZ black holes. Below or above this critical charge, the black hole is always nonextreme, which is shown in Fig. 2b. For $m > 1$, it is clear from Fig. 2c that there are always two horizons enveloping the central singularity and the black hole is nonextreme.

We further define the coordinate difference $R = r_+ - r_-$ between the inner and outer horizons to show its dependence on the parameter q for different chosen mass values in Fig. 3a. When the black hole geometrical mass is smaller than one ($m < 1$), there will be two horizons protecting the central singularity when the black hole charge is small. These two horizons approach each other with the increase of the black hole charge and the nonextreme black hole becomes extreme at $q = q_1$. When the charge parameter is between q_1 and q_2, there is no root for the metric function $f(r)$ and the black

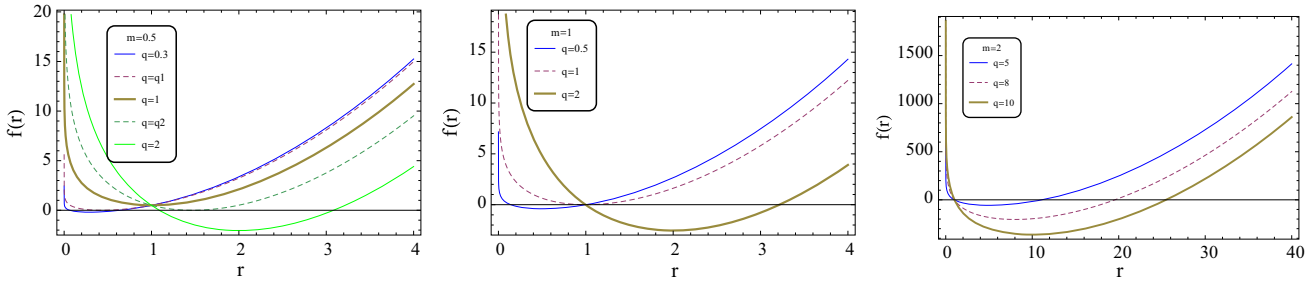

(a) $m = 0.5$ **(b)** $m = 1$ **(c)** $m = 2$

Fig. 2 The behaviors of $f(r)$ for different values of q when $m = 0.5$, 1 and 2

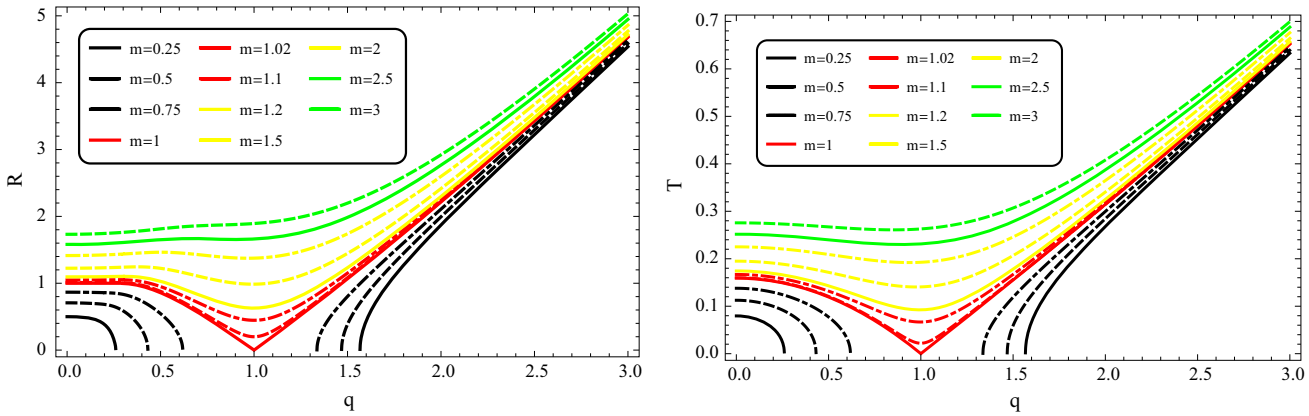

(a) R vs q **(b)** T vs q

Fig. 3 The behaviors of distance R between inner and outer horizons (*left*) and the temperature T (*right*) of charged BTZ black hole

hole does not exist. At $q = q_2$ for the chosen m value smaller than one, there is only one black hole horizon to appear to envelop the singularity again. The difference between event and Cauchy horizons becomes bigger when the black hole is more charged when $q > q_2$. When m approaches one from below, we see from Fig. 3a that q_1 and q_2 approach each other. They finally merge when $m = 1$ and only one extreme charged BTZ black hole exists for $q = 1$. Below $q = 1$, with the increase of the electric charge, the two horizons become closer to each other, degenerate finally at $q = 1$. But when above $q = 1$, the horizons can separate again when q grows and the black hole becomes more nonextreme. In the case when $m > 1$, the two horizons will never degenerate so that the black hole is always nonextreme. There exists a turning point of the mass value m_r. In the range $1 < m < m_r$, the two horizons can come closer to each other and then separate away with the increase of q, while when $m > m_r$, the distance between the two horizons of the black hole will increase monotonically.

We can calculate the charged BTZ black hole temperature,

$$T = \frac{f'(r_+)}{4\pi} = \frac{1}{2\pi}\left(\frac{r_+}{L^2} - \frac{q^2}{r_+}\right), \tag{15}$$

which is shown in Fig. 3b. The black hole temperature confirms the property we disclosed in the spacetime structure. When the black hole mass is small ($m < 1$), the black hole temperature decreases to zero with the increase of the black hole charge from 0 to q_1. When the charge is big enough ($q \geq q_2$), the black hole can exist and the temperature will rise from zero. When $m = 1$, the temperature decreases to zero at $q = 1$ and then rises with the increase of charge q. For $m > 1$, we see from Fig. 3b that there exists a turning point of the mass m_t, when $1 < m < m_t$, with the increase of the electric charge, the temperature will first decrease and then increase but the minimum of the temperature is always above zero. When $m > m_t$, the temperature increases monotonically with the increase of the electric charge.

We can clearly see that the qualitative behavior of T is closely related to R.

2.2 Nonlinearly charged BTZ black holes

The metric function of nonlinearly BI charged BTZ black hole is

$$f(r) = \frac{r^2}{l^2} - m + 2r^2\beta^2\left(1 - \Gamma\right)$$

$$+q^2\left[1-2\ln\left(r\frac{(1+\Gamma)}{2l}\right)\right]. \tag{16}$$

When $\beta\to\infty$, the results reduce to that presented in the above subsection. When β becomes smaller, the nonlinearity becomes stronger.

We repeat the discussion above to examine the spacetime structure for the nonlinearly charged BTZ black hole. The location of the horizon and the extreme condition are described by

$$f(r_+)=\frac{r_+^2}{l^2}-m_{\rm ext}+2r_+^2\beta^2\left(1-\Gamma_+\right)+q_{\rm ext}^2\left[1-2\ln\left(r_+\frac{(1+\Gamma_+)}{2l}\right)\right]=0, \tag{17}$$

and

$$f'(r_+)=\frac{2r_+^2\beta^2\left(1+\Gamma_+\right)+2q_{\rm ext}^2\left(1-2l^2\beta^2\Gamma_+\right)}{l^2\beta^2 r_+\left(1+\Gamma_+\right)\Gamma_+}=0, \tag{18}$$

where we can find the relation between $q_{\rm ext}$ and $m_{\rm ext}$ in the form

$$q_{\rm ext}^2-2q_{\rm ext}^2\ln\frac{q_{\rm ext}}{2L\beta}\sqrt{1+4l^2\beta^2}=m_{\rm ext}. \tag{19}$$

From Fig. 4, we see that there always exists a maximum value for the left-hand side of Eq. (19). This maximum value

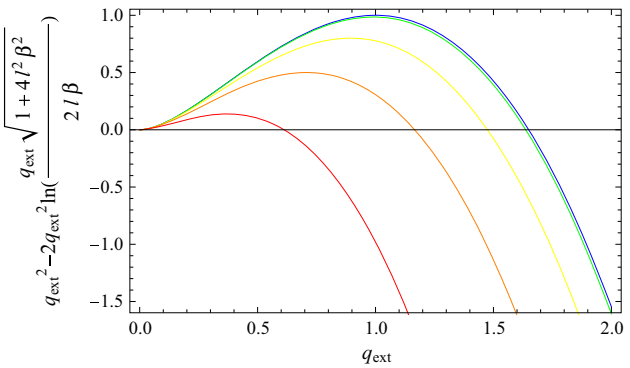

Fig. 4 The behaviors of the left-hand side of Eq. (19) versus q for $\beta=0.2, 0.5, 1, 4$, and infinity, respectively, from below to the up lines, where we take $l=1$

$4l^2\beta^2/\left(1+4l^2\beta^2\right)$ happens at $q_{\rm ext}=2l\beta/\sqrt{1+4l^2\beta^2}$. When $m=4l^2\beta^2/\left(1+4l^2\beta^2\right)$, there is only one solution q_1 which can make the black hole extreme. For $m<4l^2\beta^2/\left(1+4l^2\beta^2\right)$, there are two solutions q_1 and q_2 which satisfy the extreme black hole condition. Interestingly, q_1 and q_2 can become closer when the nonlinearity is increased in the electromagnetic field. When $m>4l^2\beta^2/\left(1+4l^2\beta^2\right)$, the extreme condition cannot be satisfied so that the black hole is always nonextreme.

To display the property more clearly, we again plot in Fig. 5 the behavior of the distance between the inner and the outer horizons R with respect to q for $m=0.25$, 1 and 2, respectively. For $m<1$ ($m=0.25$), we find that with the decrease of β, the two extreme values of the charge q get closer to each other, become one and then disappear. This means that when the nonlinearity in the electromagnetic field is strong enough, there is no extreme charged BTZ black hole. For $m=1$, the extreme black hole only exists when the gravity is coupled to the standard Maxwell field. For gravity coupled to the BI field, when the nonlinearity is not strong enough, the two horizons of the black hole can approach to each other first and then separate with the increase of the electric charge. But they cannot merge. When the electromagnetic field is strongly nonlinear, the difference between two horizons always becomes bigger with the increase of the black hole charge. For $m>1$, the influence of the nonlinearity is similar to that described for $m=1$ case.

The behavior of Hawking temperature T for the nonlinearly charged BTZ black holes is shown in Fig. 6. It gives us qualitatively the similar behavior as we discussed for R. Compared with the linearly charged BTZ black hole, the nonlinearity in the electromagnetic field makes the Hawking temperature higher and it is more difficult to reach zero temperature in the nonlinearly charged BTZ black holes.

3 Thermodynamical phase transitions

Thermodynamics of the BTZ black holes have been discussed in [8]. More references can be found in reviews [3,7].

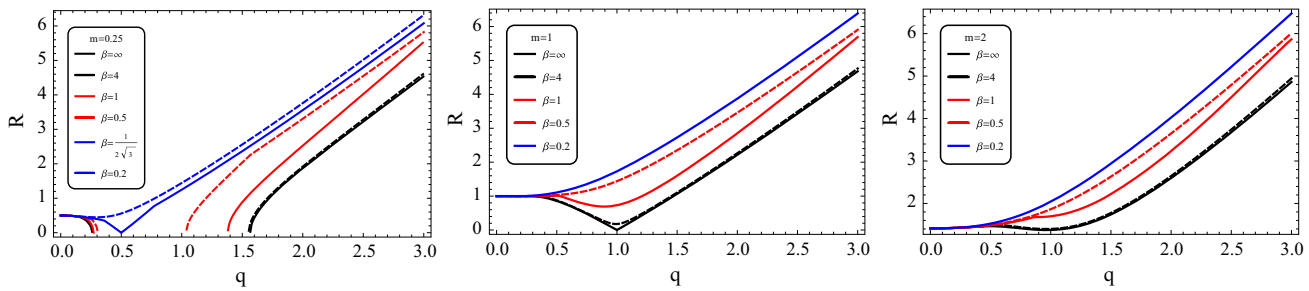

(a) $m=0.25$ **(b)** $m=1$ **(c)** $m=2$

Fig. 5 The distance R between inner and outer horizons for $m=0.25$, 1 and 2 for nonlinearly charged BTZ black holes

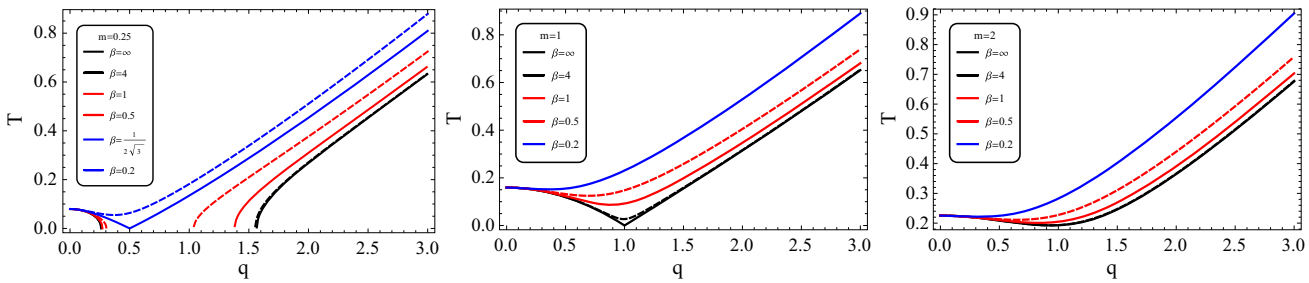

(a) $m = 0.25$ **(b)** $m = 1$ **(c)** $m = 2$

Fig. 6 The behavior of Hawking temperature T for $m = 0.25$, 1 and 2 for nonlinearly charged black holes

Most studies were focused on the BTZ black holes where gravity minimally coupled to matter fields. For the charged BTZ black holes, the first law of thermodynamics was constructed in [19], the entropy was examined in [20–22], the mass bound and thermodynamical behavior was investigated in [23] and the phase transition was studied in [24]. Recently the thermodynamical stability of the charged BTZ black hole was investigated in [10] by the method of examining the heat capacity first proposed by Davies [25–27]. The extension was performed to the nonlinearly charged BTZ black holes [28].

Here we are going to examine the thermodynamical phase transition in the charged BTZ black holes more carefully. It was argued in [12] that the heat capacity cannot be the true character to mark the phase transition, because there is no sharp change in physical properties at the point of the phase transition obtained from the heat capacity.

Besides, the comparison of the free energy of two competing configurations are often used in the context of first-order phase transition, such as the Hawking–Page phase transition, which describes the competition between a pure anti-de Sitter spacetime and an AdS black hole spacetime. However, the phase transition we studied is between non-extremal and extremal black holes. This is a second-order phase transition. So we turn to using the Landau–Lifshitz theory of thermodynamical perturbations. Employing the Landau–Lifshitz theory of thermodynamic fluctuations, the fluctuations in the rate of change of mass, angular momentum and other relevant quantities of different black holes were examined and it was found that some second moments in the fluctuation of relevant quantities diverge when the black holes become extreme, which marks the occurrence of the second-order phase transition. Below we will further use the Landau–Lifshitz theory to study the phase transition in the charged BTZ black holes.

According to Landau–Lifshitz theory [29], in a fluctuation–dissipative process, the flux $\dot{X}_i$ (dot shows temporal derivative) of a given thermodynamic quantity X_i is expressed by

$$\dot{X}_i = -\sum_j \Gamma_{ij}\chi_j, \tag{20}$$

where Γ_{ij} and χ_i are the phenomenological transport coefficients and thermodynamic force conjugate to the flux $\dot{X}_i$, respectively. Also, the entropy production rate is given by

$$\dot{S} = \sum_i \pm\chi_i \dot{X}_i. \tag{21}$$

The second moments in the fluctuations of the fluxes read

$$\left\langle \delta\dot{X}_i \delta\dot{X}_j \right\rangle = \left(\Gamma_{ij} + \Gamma_{ji}\right)\delta_{ij}, \tag{22}$$

where the angular brackets denote the mean value with respect to the steady state and the fluctuations $\delta\dot{X}_i$ are the spontaneous deviations from the steady state value $\left\langle \dot{X}_i \right\rangle$ (we set $k_B = 1$). The Kronecker δ_{ij} in Eq. (22) is to guarantee that correlations vanish when two fluxes are independent. We can obtain the rate of entropy production,

$$\begin{aligned}\dot{S}(M, Q) &= \left(\frac{\partial S}{\partial M}\right)_Q \dot{M} + \left(\frac{\partial S}{\partial Q}\right)_M \dot{Q} \\ &= \frac{\dot{M}}{T} - \frac{\dot{Q}}{T}\left(\frac{\partial M}{\partial Q}\right)_S \\ &= \frac{\dot{M}}{T} - \frac{U\dot{Q}}{T},\end{aligned} \tag{23}$$

where we have used

$$T = \left(\frac{\partial M}{\partial S}\right)_Q, \quad U = \left(\frac{\partial M}{\partial Q}\right)_S, \tag{24}$$

and

$$\left(\frac{\partial M}{\partial S}\right)_Q \left(\frac{\partial S}{\partial Q}\right)_M \left(\frac{\partial Q}{\partial M}\right)_S = -1, \tag{25}$$

in which S, M and Q are entropy, total mass and total charge of the black hole defined as [10]

$$S = \frac{\pi r_+}{2}, \quad Q = \frac{q}{2} \text{ and } M = \frac{m}{8}, \tag{26}$$

and U is the electric potential energy. Using Eqs. (11), (24) and (26), one can calculate the temperature and the electric potential energy as

$$T=\begin{cases}\frac{S}{\pi^2 l^2}-\frac{Q^2}{S} & \text{LM},\\ \frac{S}{\pi^2 l^2}-\frac{Q^2}{S}+\frac{2S\beta^2}{\pi^2}\left(1-\Gamma_S\right)+\frac{Q^2}{S\Gamma_S}+\frac{\pi^2 Q^4}{\beta^2 S^3\Gamma_S(1+\Gamma_S)} & \text{BI},\end{cases}$$

and

$$U=\begin{cases}-2Q\ln\left(\frac{2S}{\pi l}\right) & \text{LM},\\ -2Q\ln\left(\frac{S}{\pi l}\left(1+\Gamma_S\right)\right)+Q\left(1-\Gamma_S^{-1}\right)-\frac{\pi^2 Q^3}{\beta^2 S^2\Gamma_S(1+\Gamma_S)} & \text{BI},\end{cases}$$

where $\Gamma_S=\sqrt{1+Q^2\pi^2/\left(S^2\beta^2\right)}$. It is worthwhile to mention that for the extreme black hole case where $f'(r_+)=0$, the Hawking temperature vanishes since $T=f'(r_+)/4\pi$.

The rate of the mass loss is [30,31]

$$\frac{\mathrm{d}M}{\mathrm{d}t}=-b\alpha\sigma T^3+U\frac{\mathrm{d}Q}{\mathrm{d}t}. \tag{27}$$

The first term on the right side of (27) exhibits the thermal mass loss due to Hawking radiation. Note that the power of the temperature is dimension-dependent. This term is just the Stefan–Boltzmann law, in which b denotes the radiation constant. The constant α is dependent on the number of species of massless particles and the quantity σ is the geometrical optics cross-section. The second term on the right side of Eq. (27) is due to the mass loss of charged particles. In fact, It is the same term as appears in the first law of black hole mechanics, namely $U\mathrm{d}Q$.

According to what described and calculated above, we can obtain the correlation functions or the second moments of the corresponding thermodynamical quantities as

$$\begin{aligned}\left\langle\delta\dot{M}\delta\dot{M}\right\rangle&=-2T\dot{M},\left\langle\delta\dot{Q}\delta\dot{Q}\right\rangle\\&=-\frac{2T\dot{Q}}{U},\left\langle\delta\dot{M}\delta\dot{Q}\right\rangle=U\left\langle\delta\dot{Q}\delta\dot{Q}\right\rangle,\end{aligned} \tag{28}$$

$$\begin{aligned}\left\langle\delta\dot{S}\delta\dot{M}\right\rangle&=\frac{1}{T}\left\langle\delta\dot{M}\delta\dot{M}\right\rangle-\frac{U}{T}\left\langle\delta\dot{M}\delta\dot{Q}\right\rangle\\&=\frac{1}{T}\left\langle\delta\dot{M}\delta\dot{M}\right\rangle-\frac{U^2}{T}\left\langle\delta\dot{Q}\delta\dot{Q}\right\rangle=-2\dot{M}+2U\dot{Q},\end{aligned} \tag{29}$$

$$\begin{aligned}\left\langle\delta\dot{S}\delta\dot{Q}\right\rangle&=\frac{1}{T}\left\langle\delta\dot{M}\delta\dot{Q}\right\rangle-\frac{U}{T}\left\langle\delta\dot{Q}\delta\dot{Q}\right\rangle\\&=\frac{U}{T}\left\langle\delta\dot{Q}\delta\dot{Q}\right\rangle-\frac{U}{T}\left\langle\delta\dot{Q}\delta\dot{Q}\right\rangle=0,\end{aligned} \tag{30}$$

$$\begin{aligned}\left\langle\delta\dot{S}\delta\dot{S}\right\rangle&=\frac{1}{T^2}\left\langle\delta\dot{M}\delta\dot{M}\right\rangle+\frac{U^2}{T^2}\left\langle\delta\dot{Q}\delta\dot{Q}\right\rangle\\&\quad-\frac{2U}{T^2}\left\langle\delta\dot{M}\delta\dot{Q}\right\rangle=\frac{1}{T^2}\left\langle\delta\dot{M}\delta\dot{M}\right\rangle-\frac{U^2}{T^2}\left\langle\delta\dot{Q}\delta\dot{Q}\right\rangle\\&=-\frac{2\dot{M}}{T}+\frac{2U\dot{Q}}{T}=\frac{\left\langle\delta\dot{S}\delta\dot{M}\right\rangle}{T},\end{aligned} \tag{31}$$

$$\begin{aligned}\left\langle\delta\dot{T}\delta\dot{T}\right\rangle&=M_{SS}^2\left\langle\delta\dot{S}\delta\dot{S}\right\rangle+M_{SQ}^2\left\langle\delta\dot{Q}\delta\dot{Q}\right\rangle+2M_{SS}M_{SQ}\left\langle\delta\dot{S}\delta\dot{Q}\right\rangle\\&=M_{SS}^2\left\langle\delta\dot{S}\delta\dot{S}\right\rangle+M_{SQ}^2\left\langle\delta\dot{Q}\delta\dot{Q}\right\rangle,\end{aligned} \tag{32}$$

$$\begin{aligned}\left\langle\delta\dot{S}\delta\dot{T}\right\rangle&=\frac{M_{SS}}{T}\left\langle\delta\dot{S}\delta\dot{M}\right\rangle+\frac{M_{SQ}}{T}\left\langle\delta\dot{M}\delta\dot{Q}\right\rangle-\frac{UM_{SS}}{T}\left\langle\delta\dot{S}\delta\dot{Q}\right\rangle\\&\quad-\frac{UM_{SQ}}{T}\left\langle\delta\dot{Q}\delta\dot{Q}\right\rangle=M_{SS}\left\langle\delta\dot{S}\delta\dot{S}\right\rangle.\end{aligned} \tag{33}$$

Note that, for calculating $\left\langle\delta\dot{T}\delta\dot{T}\right\rangle$ and $\left\langle\delta\dot{S}\delta\dot{T}\right\rangle$, we have used

$$\dot{T}(S,Q)=\left(\frac{\partial T}{\partial S}\right)_Q\dot{S}+\left(\frac{\partial T}{\partial Q}\right)_S\dot{Q}=M_{SS}\dot{S}+M_{SQ}\dot{Q}, \tag{34}$$

in which $M_{XY}=\partial^2 M/\partial X\partial Y$. Since T vanishes for the extreme black hole case, the second moments $\left\langle\delta\dot{S}\delta\dot{S}\right\rangle,\left\langle\delta\dot{T}\delta\dot{T}\right\rangle$ and $\left\langle\delta\dot{S}\delta\dot{T}\right\rangle$ diverge there. The divergence of the second moment means that the fluctuation is tremendous which breaks down the rigorous meaning of thermodynamical quantities. This is just the characteristic of the point of the phase transition. This property holds for the nonlinearly charged BTZ black hole as well.

4 The dynamical perturbations

It is an interesting question how we can examine the phase transition through physical phenomena. Hiscock and Weems's argument tells us that the Hawking radiation is not exactly zero when the black hole temperature vanishes [24]. This makes the attempt to indicate of the second-order black hole phase transition through different radiation properties fade. In this section we are going to explore the properties of the dynamical perturbations in the charged BTZ black hole background. We will examine the behavior of quasi-normal modes (QNMs) of scalar perturbations, and will argue that the dynamical perturbation behavior can serve as a new probe of the phase transition between the extreme and nonextreme black holes.

QNM of black holes does not depend on perturbation fields outside black holes. Instead, it only depends on properties of the background spacetime. Thus QNMs can reflect the dynamical properties of black holes. It was argued in [32] that the QNMs of the electromagnetic perturbations can give evidence of a second-order phase transition of a topological black hole to a hairy configuration. Further supports that the QNMs can be probes of the phase transition were provided in [33,34]. In a recent paper, it was reported that the signature of the Van der Waals like small-large charged AdS black hole phase transition can also be observed in QNM [35]. It is of interest to generalize the previous studies to investigate the dynamical perturbations in the charged BTZ black holes and examine whether the QNMs of the perturbation can again be a physical indication of the thermodynamical phase transition.

In calculating the QNMs, we have tried three different numerical methods [6], namely the Horowitz–Hobeny method, the Shooting method and the asymptotic iteration

method (AIM). We found that the AIM is the most precise and efficient method, especially when the black hole approaches extremality. In the following we will introduce the AIM method first and present the numerical results.

AIM was first used to solve eigenvalue problems of the second-order homogeneous linear differential equations [36], and then applied to the case of black hole QNMs. Considering the second-order homogeneous linear differential equation

$$\chi'' = \lambda_0(x)\chi' + s_0(x)\chi, \tag{35}$$

where $\lambda_0(x)$ and $s_0(x)$ are smooth functions in some interval $[a, b]$ and taking the derivative of Eq. (35) with respect to x, we obtain the following equation:

$$\chi''' = \lambda_1(x)\chi' + s_1(x)\chi, \tag{36}$$

where

$$\lambda_1(x) = \lambda_0'(x) + s_0(x) + \lambda_0^2(x), \quad \text{and} \quad s_1 = s_0'(x) + s_0(x)\lambda_0(x). \tag{37}$$

Repeating this step iteratively, we can obtain the $(n+2)$th derivatives,

$$\chi^{(n+2)} = \lambda_n(x)\chi' + s_n(x)\chi, \tag{38}$$

where

$$\lambda_n(x) = \lambda_{n-1}'(x) + s_{n-1}(x) + \lambda_0(x)\lambda_{n-1}(x), \quad \text{and} \quad s_n(x) = s_{n-1}'(x) + s_0(x)\lambda_{n-1}(x). \tag{39}$$

For sufficiently large n, the asymptotic aspect of the method is introduced as [37]

$$\frac{s_n(x)}{\lambda_n(x)} = \frac{s_{n-1}(x)}{\lambda_{n-1}(x)}. \tag{40}$$

The QNMs can be derived from the above "quantization condition". However, the derivatives of $\lambda_n(x)$ and $s_n(x)$ in each iteration can slow down the numerical implementation of the AIM considerably and also lead to precision problems. These drawbacks were overcome in the improved version of AIM [38]. $\lambda_n(x)$ and $s_n(x)$ can be expanded in Taylor series around the point ξ at which the AIM is performed,

$$\lambda_n(\xi) = \sum_{i=0}^{\infty} c_n^i (x-\xi)^i, \quad \text{and} \quad s_n(x) = \sum_{i=0}^{\infty} d_n^i (x-\xi)^i. \tag{41}$$

Here c_n^i and d_n^i are the ith Taylor coefficients of $\lambda_n(\xi)$ and $s_n(\xi)$, respectively. Substituting these expansions into Eq. (39), we obtain a set of recursion relations for the coefficients,

$$c_n^i = (i+1)c_{n-1}^{i+1} + d_{n-1}^i + \sum_{k=0}^{i} c_0^k c_{n-1}^{i-k}, \quad \text{and}$$

$$d_n^i = (i+1)d_{n-1}^{i+1} + \sum_{k=0}^{i} d_0^k c_{n-1}^{i-k}. \tag{42}$$

Consequently, the "quantization condition" can be expressed as

$$d_n^0 c_{n-1}^0 - d_{n-1}^0 c_n^0 = 0, \tag{43}$$

which no longer requires the derivative operator. Both the accuracy and the speed of the AIM computation are greatly improved by this change.

Now we apply this method to charged BTZ black holes. The massless Klein–Gordon equation is

$$\nabla^\nu \nabla_\nu \Psi = 0. \tag{44}$$

The solution of (44) can be considered in the form of

$$\Psi = e^{-i\omega t} R(r) Y(\theta), \tag{45}$$

which enables us to decompose the differential equation (44) into two parts:

$$\frac{\partial^2 Y(\theta)}{\partial \theta^2} = 0, \tag{46}$$

$$R''(r) + \left[\frac{f'(r)}{f(r)} + \frac{1}{r}\right] R'(r) + \frac{\omega^2 R(r)}{f(r)^2} = 0, \tag{47}$$

where we set the separation constant to zero. With the definitions

$$R(r) = \frac{\psi(r)}{\sqrt{r}} \tag{48}$$

and

$$\mathrm{d}r_* = \frac{\mathrm{d}r}{f(r)}, \tag{49}$$

where r_* is the tortoise coordinate, we can rewrite (47) in the Schrödinger form,

$$\frac{\partial^2 \psi}{\partial r_*^2} + \left(\omega^2 - V(r)\right)\psi = 0, \tag{50}$$

where

$$V(r) = \frac{f(r)f'(r)}{2r} - \frac{f(r)^2}{4r^2}. \tag{51}$$

We take a coordinate transformation $\xi = 1 - r_+/r$. At infinity $r \to \infty, \xi \to 1$ and at horizon $r \to r_+, \xi \to 0$ and therefore we can choose the point ξ between 0 and 1. Applying $\xi = 1 - r_+/r$, Eq. (50) turns to

$$\frac{\partial^2 \psi}{\partial \xi^2} = \lambda_0(\xi)\frac{\partial \psi}{\partial \xi} + s_0(\xi)\psi. \tag{52}$$

We will express λ_0 and s_0 for linearly and nonlinearly charged cases separately in the following of this section and apply AIM to calculating of the QNMs corresponding to each case.

4.1 Linearly charged case

In the linearly charged case we have

$$\lambda_0(\xi) = \frac{1}{1-\xi}\left[3 + \frac{2ik\omega\,(1-\xi)}{\xi}\right] + \frac{2l^2\,(1-\xi)^2\left(m - q^2 + 2q^2\ln\frac{r_+}{l(1-\xi)}\right)}{l^2 m\,(1-\xi)^2 - r_+^2 + 2l^2q^2\,(1-\xi)^2\ln\frac{r_+}{l(1-\xi)}}, \tag{53}$$

$$\begin{aligned} s_0(\xi) = &-\frac{1}{4\,(1-\xi)^4}\left[3\,(1-\xi)^2 - \frac{12ik\omega\,(1-\xi)^3}{\xi} - \frac{4k\omega\,(k\omega - i)\,(1-\xi)^4}{\xi^2}\right] \\ &-\frac{1}{4\,(1-\xi)^4}\left[\frac{4l^2\,(1-\xi)^4\,(2ik\omega + \xi\,(3 - 2ik\omega))\left(m - q^2 + 2q^2\ln\frac{r_+}{l(1-\xi)}\right)}{\xi\left(l^2 m\,(1-\xi)^2 - r_+^2 + 2l^2q^2\,(1-\xi)^2\ln\frac{r_+}{l(1-\xi)}\right)}\right] \\ &-\frac{r_+^2}{(1-\xi)^4}\left[\frac{\left(\omega^2 - \frac{1}{4l^4 r_+^2(1-\xi)^2}\right)\left(r_+^2 - l^2 m\,(1-\xi)^2 - 2l^2q^2\,(1-\xi)^2\ln\frac{r_+}{l(1-\xi)}\right)}{\left(m - \frac{r_+^2}{l^2(1-\xi)^2} + 2q^2\ln\frac{r_+}{l(1-\xi)}\right)^2}\right] \\ &\times\left(3r_+^2 + l^2\left(m - 4q^2\right)(1-\xi)^2 + 2l^2q^2\,(1-\xi)^2\ln\frac{r_+}{l\,(1-\xi)}\right), \end{aligned} \tag{54}$$

where $k = \left[f'(r_+)\right]^{-1}$ and ω is the quasi-normal frequency. Substituting (53) and (54) into the (52), we can obtain the QNMs of charged BTZ black holes in the presence of Maxwell electrodynamic field by using (42) and (43).

Calculations show that the real part of QNMs (ω_{R}) is always zero. So in the charged BTZ black hole there is no oscillation of the dynamic perturbation. This is consistent with the result found in the neutral BTZ black hole [39]. The dynamical perturbation only decays with the relaxation time scale measured by the imaginary part of QNMs (ω_{I}), whose dependence on the model parameters is shown in Fig. 7. For the nonextreme black hole in the allowed parameters range discussed above, the dynamical perturbation will die out which ensures the stability of the black hole spacetime. But when the black hole approaches the extreme case, ω_{I} becomes less negative and the decay of the perturbation becomes slower. In the extreme case, ω_{I} becomes zero. This indicates that for the extreme black hole, the perturbation will never die out which makes the black hole spacetime unstable. For the cases $m < 1$, $q \geq q_2$ and $m = 1$, $q \geq 1$, with the increase of q, we observe that the perturbation can decay faster, which makes the black hole even more stable. When $m > 1$, the black hole can never become extreme and the ω_{I} is always negative.

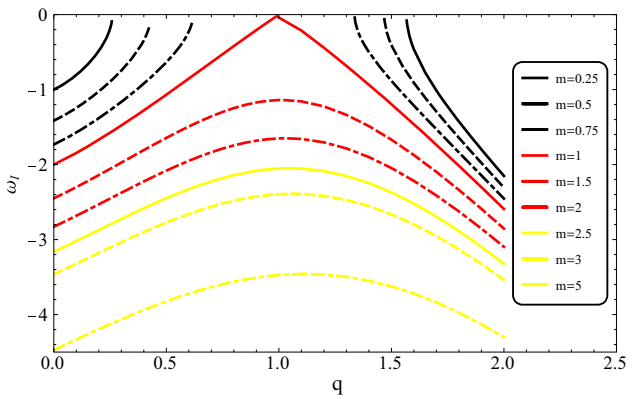

Fig. 7 The behavior of imaginary parts of QNMs (ω_{I}) with respect to q

It is interesting that the QNMs behavior exactly reflects what we discussed for the spacetime property. Especially we find that when the black hole phase transition happens, the dynamical perturbation presents us a drastically different property. Nonextreme black hole can always be stable with the decay of the dynamical perturbation, while the perturbation on the extreme black hole background can persist which makes the extreme black hole quasi-stable. This serves as another marking of the phase transition and indicates different properties of different phases in the black hole.

4.2 Nonlinearly charged case

In the nonlinearly BI charged case, we have

$$\lambda_0(\xi) = \frac{3\xi + 2ik\omega - 2ik\omega\xi}{\xi - \xi^2} + \frac{2(1-\xi)\left(m - q^2 + 2q^2 B(\xi)\right)}{\left(m-q^2\right)\left(1 - 2\xi + \xi^2\right) - r_+^2\left(2\beta^2 - 1\right) + 2r_+^2\beta^2 A(\xi) + 2q^2(1-\xi)^2 B(\xi)}, \tag{55}$$

$$\begin{aligned} s_0(\xi) = & -\frac{1}{(1-\xi)^2}\left[1 - \frac{3ik\omega(1-\xi)}{\xi} - \frac{k\omega(1-\xi)^2(k\omega - i)}{\xi^2}\right] \\ & - \frac{(2ik\omega + \xi(3 - 2ik\omega))\left(m - q^2 + 2q^2 B(\xi)\right)}{\xi\left[\left(m-q^2\right)\left(1 - 2\xi + \xi^2\right) - r_+^2\left(2\beta^2 - 1\right) + 2r_+^2\beta^2 A(\xi) + 2q^2(1-\xi)^2 B(\xi)\right]} \\ & - \frac{\omega^2}{r_+^2\left(-1 + 2\beta^2(-1 + A(\xi)) + \frac{m(1-\xi)^2}{r_+^2} + \frac{q^2(1-\xi)^2}{r_+^2}(-1 + 2B(\xi))\right)^2} \\ & + \frac{r_+^2\left(-1 - 2\beta^2 + 2\beta^2 A(\xi)\right)}{(1-\xi)^2\left[\left(m-q^2\right)\left(1 - 2\xi + \xi^2\right) - r_+^2\left(2\beta^2 - 1\right) + 2r_+^2\beta^2 A(\xi) + 2q^2(1-\xi)^2 B(\xi)\right]}, \end{aligned} \tag{56}$$

where

$$A(\xi) = \sqrt{1 + \frac{q^2(1-\xi)^2}{r_+^2\beta^2}}, \quad \text{and} \quad B(\xi) = \ln\frac{r_+(1 + A(\xi))}{2(1-\xi)}. \tag{57}$$

Substituting (55) and (56) into the (52), we can calculate the QNMs of BI charged BTZ black holes by using (42) and (43).

Again the real part of QNMs (ω_{R}) vanishes indicating that there is no oscillation of the perturbation. The decay time scale of the perturbation can be measured by the imaginary part of ω_I which is shown in Fig. 8. This behavior is similar to that of the linearly charged case.

For the nonextreme black hole, the spacetime is always stable, since the dynamic perturbation will die out finally. When the nonextreme black hole approaches extreme with the increase of the electric charge, the perturbation will die out more slowly, since the ω_{I} becomes less negative. For the extreme black hole, ω_{I} is zero which indicates that for the extreme black hole background, the perturbation will persist and will not die out. Compared with the linearly charged BTZ black hole case, we have observed that the nonlinearity introduced here helps to protect the stability of the black hole. Increasing of the nonlinearity, the ω_{I} becomes more negative for the same parameters m and q case. This agrees with the observation in the four-dimensional BI AdS black hole [40]. The QNMs behavior reflects the spacetime properties discussed above. Interestingly we again witnessed that the dynamic perturbation can be a signature to probe the phase transition in the system. We see the evidence that two phases, the nonextreme and extreme black holes have different dynamical behaviors. This actually supports the phase transition results obtained in the previous section.

5 Summary and conclusions

In this paper, we have carefully examined the spacetime properties of BTZ black holes in Maxwell field and Born–Infeld field. We found new, rich spacetime structures of the black hole when the model parameters are varied. These special spacetime properties determine the conditions of phase transition. For a charged BTZ black hole with mass in a small value regime, $0 < m < 1$, the black hole can evolve from nonextreme to extreme black hole when the charge of the black hole increases from zero to some q_1. When the charge of the black hole increases further, there will be no black hole solution. But when the charge parameter becomes as big as some q_2, an extreme black hole appears and this extreme black hole will become nonextreme with the further increase of the charge parameter. The difference between q_1 and q_2 will become smaller with the increase of m and q_1, q_2 will degenerate when $m = 1$. But when the mass parameter is bigger than 1, the black hole will always be nonextreme, no matter how much we increase the charge parameter. Generalizing the discussion to the nonlinear charged BTZ black holes, we find the qualitative behaviors in the structures of black hole persist when we have the case of the BTZ black hole with nonlinear Born–Infeld electromagnetic field.

Furthermore we have studied the thermodynamical phase transition in the charged BTZ black hole background. Instead of the heat capacity, we have employed the Landau–Lifshitz theory and examined the second moments of relevant parameters in the system. We have found that some second moments

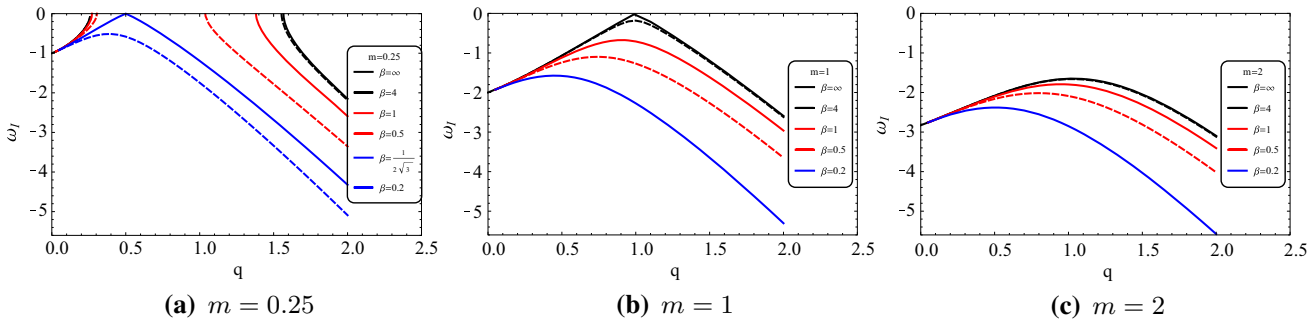

(a) $m = 0.25$ **(b)** $m = 1$ **(c)** $m = 2$

Fig. 8 The behavior of imaginary parts of QNMs ($\omega_{\rm I}$) with respect to q for nonlinearly charged case

diverge when the black hole extreme limit is reached, which indicates the break down of the rigorous meaning of thermodynamical quantities. This marks the occurrence of the thermodynamical phase transition, where some physical properties change.

To disclose more signature of the phase transition, we have calculated the QNMs for the charged BTZ black holes. The dynamical perturbation does not oscillate in the charged BTZ black hole. It only shows the decay behavior when the charged BTZ black hole is nonextreme, which shows that the perturbation outside the nonextreme black hole will finally die out so that the nonextreme charged BTZ black hole is always stable. When the nonextreme black hole evolves towards the extreme hole, the decay becomes slower. But when the extreme black hole is reached, the dynamical perturbation will not decay, it persists. This is a dangerous signal which tells us that the extreme charged BTZ black hole is easily destroyed if we add more perturbations to the system. Considering the nonlinearity of the electromagnetic field, we have observed that the nonlinearity can partially save the black hole and make the perturbation outside the black hole decay faster. The different properties of QNMs for the extreme and nonextreme charged BTZ black holes are interesting. They can serve as another probe for the phase transition between the nonextreme and extreme black holes.

We have discussed the relation between horizons and found that there exists a turning value in the mass parameter, m_r. When $m > 1$, the black hole is always nonextreme, but in the range $1 < m < m_r$, two horizons can first approach each other and then separate away with the increase of charge q, but when $m > m_r$, the difference between two horizons will become bigger monotonically when q increases. At first sight, this property looks similar to the temperature behavior, since when $m > 1$, black hole temperature also has a turning point at m_t. But we found that m_r and m_t do not coincide. The reason can be understood: the temperature is just an apparent thermodynamical quantity, it cannot reflect deep physics in the spacetime property. In the QNM behavior, we found that when the black hole horizons get closer, the perturbation around the black hole decays slower and slower. But when the difference between black hole horizons becomes bigger, the black hole becomes more nonextreme, the perturbation around the black hole decays faster. The value m_r is really the boundary parameter we can distinguish the speed of the decay of perturbations around black holes. However, this behavior change in the QNMs does not show up in m_t. This tells us that the black hole temperature is not a good index reflecting the spacetime dynamical property.

The zero temperature of the extreme black hole is a thermodynamical indication of the occurrence of a second-order phase transition between nonextreme and extreme black holes [12]. But this is not a direct reason for the behavior of QNMs. The vanishing decay of the dynamical perturbation is an intrinsic result of the phase transition happening between nonextreme and extreme black holes. It is not caused directly by the zero temperature of the black hole.

Acknowledgements This work was supported in part by NNSF of China. MKZ would like to thank Shanghai Jiao Tong University for the warm hospitality during his visit. This work has been supported financially by Research Institute for Astronomy and Astrophysics of Maragha (RIAAM). We thank Yen Chin Ong for useful discussions.

Funded by SCOAP[3].

References

1. M. Banados, C. Teitelboim, J. Zanelli, The black hole in three-dimensional space-time. Phys. Rev. Lett. **69**, 1849 (1992). arXiv: hep-th/9204099
2. E. Witten, *Three-Dimensional Gravity Revisited*. arXiv:0706.3359 [hep-th]
3. S. Carlip, Conformal field theory, (2+1)-dimensional gravity, and the BTZ black hole. Class. Quant. Grav. **22**, R85 (2005). arXiv: gr-qc/0503022
4. D. Birmingham, I. Sachs, S.N. Solodukhin, Conformal field theory interpretation of black hole quasinormal modes. Phys. Rev. Lett. **88**, 151301 (2002). arXiv: hep-th/0112055

5. B. Wang, Perturbations around black holes. Braz. J. Phys. **35**, 1029 (2005). arXiv: gr-qc/0511133
6. R.A. Konoplya, A. Zhidenko, Quasinormal modes of black holes: from astrophysics to string theory, Rev. Mod. Phys. **83**, 793 (2011). arXiv:1102.4014 [gr-qc]
7. S. Carlip, The (2+1)-dimensional black hole. Class. Quant. Grav. **12**, 2853 (1995). arXiv: gr-qc/9506079
8. M. Banados, M. Henneaux, C. Teitelboim, J. Zanelli, Geometry of the (2+1) black hole. Phys. Rev. D **48**, 1506 (1993). arXiv: gr-qc/9302012
9. S.A.H. Mansoori, B. Mirza, M.D. Darareh, S. Janbaz, Entanglement thermodynamics of the generalized charged BTZ black hole. Int. J. Mod. Phys. A **31**(12), 1650067 (2016). arXiv:1512.00096 [gr-qc]
10. S.H. Hendi, S. Panahiyan, R. Mamasani, Thermodynamic stability of charged BTZ black holes: ensemble dependency problem and its solution. Gen. Rel. Grav. **47**(8), 91 (2015). arXiv:1507.08496 [gr-qc]
11. M. Born, L. Infeld, Foundations of the new field theory. Proc. R. Soc. Lond. A **144**, 425 (1934)
12. D. Pavon, J.M. Rubi, Nonequilibrium thermodynamic fluctuations of black holes. Phys. Rev. D **37**, 2052 (1988)
13. D. Pavon, Phase transition in Reissner–Nordstrom black holes. Phys. Rev. D **43**, 2495 (1991)
14. R.G. Cai, R.K. Su, P.K.N. Yu, Nonequilibrium thermodynamic fluctuations of charged dilaton black holes. Phys. Rev. D **48**, 3473 (1993)
15. C.M. Chen, S.P. Kim, I.C. Lin, J.R. Sun, M.F. Wu, Spontaneous pair production in Reissner–Nordstrom black holes. Phys. Rev. D **85**, 124041 (2012). arXiv:1202.3224 [hep-th]
16. Y.C. Ong, P. Chen, Charge loss (or the lack thereof) for AdS black holes. JHEP **1406**, 061 (2014). arXiv:1404.5215 [gr-qc]
17. S.W. Hawking, Particle creation by black holes. Commun. Math. Phys. **43**, 199 (1975). Erratum: [Commun. Math. Phys. **46** (1976) 206]
18. G.W. Gibbons, Vacuum polarization and the spontaneous loss of charge by black holes. Commun. Math. Phys. **44**, 245 (1975)
19. E.A.L. Rubio, Thermodynamics of charged BTZ black holes and effective string theory. Acta Phys. Polon. B **39**, 1349 (2008). arXiv:0710.1825 [gr-qc]
20. M. Cadoni, M. Melis, M.R. Setare, Microscopic entropy of the charged BTZ black hole. Class. Quant. Grav. **25**, 195022 (2008). arXiv:0710.3009 hep-th
21. Y.S. Myung, Y.W. Kim, Y.J. Park, Entropy function approach to charged BTZ black hole. Gen. Rel. Grav. **42**, 1919 (2010). arXiv:0903.2109 [hep-th]
22. B. Wang, E. Abdalla, Entropy of extreme three-dimensional charged black holes. Phys. Lett. B **468**, 208 (1999). arXiv: hep-th/9911005
23. M. Cadoni, C. Monni, Mass bound and thermodynamical behaviour of the charged BTZ black hole. J. Phys. Conf. Ser. **222**, 012039 (2010)
24. B. Wang, J.M. Zhu, Nonequilibrium thermodynamic fluctuations of (2+1)-dimensional black holes. Mod. Phys. Lett. A **10**(18), 1269 (1995)
25. P. C. W. Davies,"Thermodynamics of Black Holes", Proc. Roy. Soc. Lond. A **353**, 499 (1977)
26. P.C.W. Davies, Thermodynamics of black holes. Rept. Prog. Phys. **41**, 1313 (1978)
27. P.C.W. Davies, Thermodynamic phase transitions of Kerr–Newman black holes in de sitter space. Class. Quant. Grav. **6**, 1909 (1989)
28. N. Chandra, K. Khare, Dictionary based approach to edge detection. arXiv:1509.00714
29. L. Landau, E.M. Lifshitz, *Statistical Physics* (Pergamon Press, Oxford, 1980)
30. W.A. Hiscock, L.D. Weems, Evolution of charged evaporating black holes. Phys. Rev. D **41**, 1142 (1990)
31. T.R. Cardoso, A.S. de Castro, The blackbody radiation in D-dimensional universes. Rev. Bras. Ens. Fis. **27**, 559 (2005). arXiv: quant-ph/0510002
32. G. Koutsoumbas, S. Musiri, E. Papantonopoulos, G. Siopsis, Quasi-normal modes of electromagnetic perturbations of four-dimensional topological black holes with scalar hair. JHEP **0610**, 006 (2006). arXiv: hep-th/0606096
33. J. Shen, B. Wang, C.Y. Lin, R.G. Cai, R.K. Su, The phase transition and the quasi-normal modes of black holes. JHEP **0707**, 037 (2007). arXiv: hep-th/0703102
34. X.P. Rao, B. Wang, G.H. Yang, Quasinormal modes and phase transition of black holes. Phys. Lett. B **649**, 472 (2007). arXiv:0712.0645 [gr-qc]
35. Y. Liu, D.C. Zou, B. Wang, Signature of the Van der Waals like small-large charged AdS black hole phase transition in quasinormal modes. JHEP **1409**, 179 (2014). arXiv:1405.2644 [hep-th]
36. H. Ciftci, R.L. Hall, N. Saad, Perturbation theory in a framework of iteration methods. Phys. Lett. A **340**, 388 (2005)
37. H.T. Cho, A.S. Cornell, J. Doukas, T.R. Huang, W. Naylor, A new approach to black hole quasinormal modes: a review of the asymptotic iteration method. Adv. Math. Phys. **2012**, 281705 (2012). arXiv:1111.5024 [gr-qc]
38. H.T. Cho, A.S. Cornell, J. Doukas, W. Naylor, Black hole quasi-normal modes using the asymptotic iteration method. Class. Quant. Grav. **27**, 155004 (2010). arXiv:0912.2740 [gr-qc]
39. V. Cardoso, J.P.S. Lemos, Scalar, electromagnetic and Weyl perturbations of BTZ black holes: quasinormal modes. Phys. Rev. D **63**, 124015 (2001). arXiv: gr-qc/0101052
40. Y. Liu, B. Wang, Perturbations around the AdS Born–Infeld black holes. Phys. Rev. D **85**, 046011 (2012). arXiv:1111.6729 [gr-qc]